A&A 372, 945–951 (2001)
DOI: 10.1051/0004-6361:20010549

Astronomy & Astrophysics

$UBVRI$-polarimetry of the AM Herculis star RX J0203.8+2959

S. Katajainen[1], F. Scaltriti[3,⋆], V. Piirola[1], H. J. Lehto[1,2], and E. Anderlucci[3,⋆]

[1] Tuorla Observatory, Väisäläntie 20, 21500 Piikkiö, Finland
[2] Department of Physics, 21400, Turku University, Finland
[3] Osservatorio Astronomico di Torino, 10025 Pino Torinese, Italy

Received 15 December 1999 / Accepted 9 April 2001

Abstract. We present results of the first simultaneous $UBVRI$-photopolarimetric observations of the long period (4.6 hrs) AM Herculis system RX J0203.8+2959. The observed circular polarization shows both negative and positive polarization, from +7% to −5% in the B-band. A rise of the positive circular polarization is observed near the same orbital phase as a change in HR1 hardness ratio from soft to hard in the earlier ROSAT X-ray observations. The negative circular polarization is observed near orbital phases where a soft X-ray component was seen in ROSAT observations. Linear polarization pulses coincide with the sign reversal of the circular polarization, and coincide also with changes in the X-ray hardness ratio in earlier ROSAT data. The observed polarization variations favour two-pole accretion. Least square fits to the position angle curves during linear pulses suggest high orbital inclination, estimates from $i = 67^{\circ}_{-24}{}^{+21}$ to $i = 73^{\circ}_{-15}{}^{+13}$. The $UBVRI$-lightcurves show smooth variations with a broad maximum and minimum. RX J0203.8+2959 was in intermediate accretion state during observations in November 1998 ($V = 15.7 - 16.7$). The observed flux and circular polarization variations are reproduced by using constant temperature cyclotron emission models having two accretion regions and with parameters: $kT = 10$ keV, $\Lambda = 10^5$ and colatitude $\beta = 120^{\circ}-140^{\circ}$ for the negative pole, and $kT = 20$ keV, $\Lambda = 10^4$ and $\beta = 20^{\circ}-30^{\circ}$ for the main accreting positive pole, and assuming orbital inclination $i \sim 70^{\circ}$.

Key words. stars: magnetic fields – novae, cataclysmic variables – stars: individual: RX J0203.8+2959 – accretion, accretion disks – polarization

1. Introduction

The object RX J0203.8+2959 belongs to a sample of very soft X-ray sources in the ROSAT All-Sky Survey (RASS). It was preliminarily identified as an AM Herculis star by Beuermann & Thomas (1993). Schwarz et al. (1998) confirmed that RX J0203.8+2959 has properties typical for an AM Herculis star (a subclass of cataclysmic variables, CVs), with an orbital period of 4.6 hrs and brightness variations between $V = 18-15.5$. Schwarz et al. (1998) detected cyclotron emission harmonics and estimated the magnetic field strength $B \sim 38 \pm 2$ MG. The orbital period of RX J0203.8+2959 is one of the longest among all the AM Herculis stars; only two systems, V1309 Ori (7.98 hrs) and V895 Cen (4.76 hrs) have longer orbital periods. Most of the AM Herculis stars have periods below the "period gap", which occurs between 2 and 3 hours. Being one of the longest period AM Herculis systems, RX J0203.8+2959 is an important object to study the synchronization process between the primary and the secondary and the accretion mechanism in the long period ($P_{\rm orb} \geq 3$ hrs) AM Herculis stars.

Send offprint requests to: S. Katajainen,
e-mail: sekataja@astro.utu.fi

⋆ Visiting Astronomer, Complejo Astronomico El Leoncito operated under agreement between the Consejo Nacional de Investigaciones y Tecnicas de la Republica Argentina and the National Universities of La Plata, Cordoba and San Juan.

2. Observations

Our observations were carried out during 7 nights from 13/14 to 19/20 November, 1998, (JD 2451131 – 2451137) with the Turin-photopolarimeter at the 2.15 metre telescope of Complejo Astronomico El Leoncito, CASLEO in Argentina (latitude −31° 47′ 12″). The multichannel double image chopping instrument, with dichroic filters to split the light into five spectral regions for photomultipliers, follows the design principles of Piirola (1973, 1988). It provides in the U-, B-, V-, R- and I-bands simultaneous circular and linear polarimetry as well as photometry in $\lambda/4$–mode. The efficiency for the circular polarimetry is ∼70% and ∼50% for the linear polarimetry with the $\lambda/4$–retarder, and ∼100% for linear polarimetry with the $\lambda/2$–retarder. During the nights of 15/16, 16/17 and 18/19 November, 1998, the instrument was used in $\lambda/2$–mode for maximum efficiency for linear polarization data, and on the other nights (13/14, 14/15, 17/18

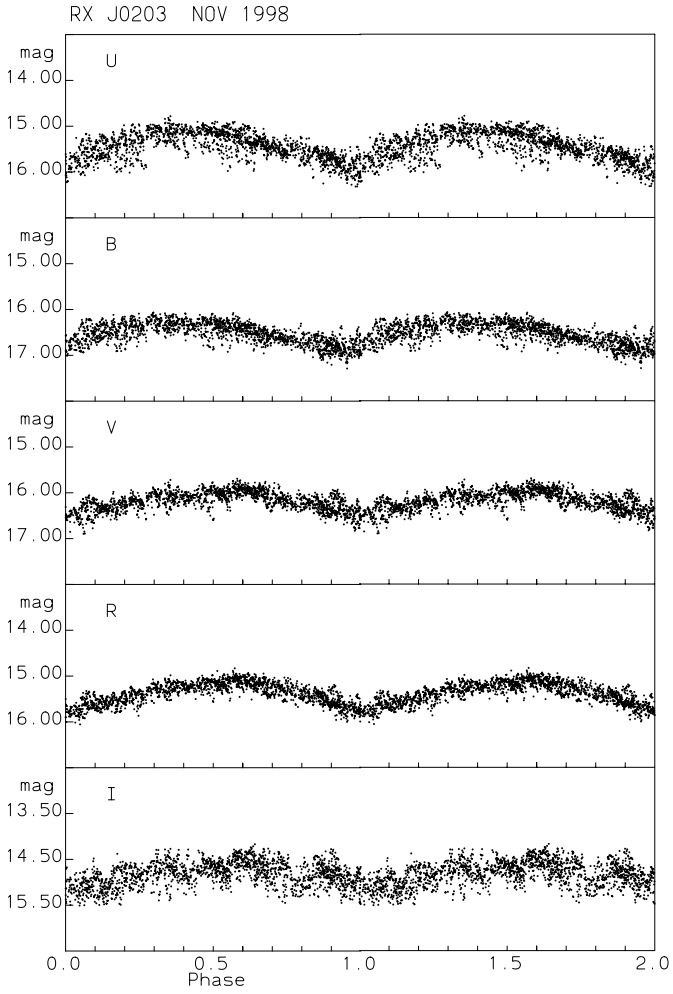

Fig. 1. Simultaneous ($UBVRI$) light curves of RX J0203.8+2959 between nights 13/14 and 19/20 November, 1998. Each point presents a single photometric measurement.

and 19/20 November, 1998) $\lambda/4$–mode was used. The sky background polarization is directly eliminated by using a calcite plate as polarizing beam splitter. The instrumental polarization and the zero-point of the position angle are determined through observations of high and low polarization standard stars. The data have been folded in Figs. 1–3 by using the ephemeris determined from V-band minima by Schwarz et al. (1998):

$$T_{\min} = HJD\ 2449243.9401(50) + E \times 0\overset{\mathrm{d}}{.}1917448(7). \quad (1)$$

2.1. Photometric UBVRI-observations

Photometric $UBVRI$-data were obtained during 7 nights (from 13/14 to 19/20, November, 1998) with time resolution of 26 s. Figure 1 presents simultaneous light curves ($UBVRI$) folded over the 4.6 hr orbital period. Light curves in Fig. 1 have been plotted twice (from phase $\Phi = 0.0$ to $\Phi = 2.0$) to illustrate the variations over the orbital period. Brightness varies between magnitudes 16 and 17 in the B- and V-bands. The range of variations is about one magnitude in all bands. The brightness level in the medium accretion state is $V = 17{-}16$ and in the high state $V = 16{-}15$, according to Schwarz et al. (1998). The broad maxima in the U- and the B-bands occur between the orbital phases $\Phi = 0.3{-}0.4$, whereas the V-, R-, and the I-bands have their maximum 0.3 phase later ($\Phi = 0.6{-}0.7$). Minima in the light curves occur between the phases $\Phi = 0.90{-}0.95$ in the U- and the B-bands, whereas the V-, R-, and I-bands have their mimima centered at the phase $\Phi = 0.0$. Schwarz et al. (1998) also reported phase dependent minima: during their observations the I-band light curve mimimum lagged the minimum in the B-band by $\sim$0.12 phase units. Small variability in the shape of the light curves from night to night, accompanied with some flickering, complicate accurate determination of times of minima. Predicted timing errors in ephemeris given by Schwarz et al. (1998) in November 1998 are $\pm$10 min ($\pm$0.04 phase units).

Due to the Northern declination, the maximum duration of the nightly runs was slightly greater than 4 hours (almost one complete cycle) and the values of air masses were between 2.1 and 2.7. We estimate that the accuracy of our photometry is 0.04 mag for the $UBVR$ bands and 0.08 mag for the I-band. The full average spread of the observations in light curves are: 0.45 mag (U), 0.30 (B), 0.30 (V), 0.27 (R), 0.55 (I). Even though we consider some uncertainty arising from an estimate of the extinction coefficients (due to the low altitude of the object), we believe that the observed spread in the curves reflects real changes in the physical phenomenona in the source.

2.2. Polarimetry

Polarimetry data, plotted from orbital phase $\Phi = 0.0$ to $\Phi = 2.0$, are shown in Fig. 2 (circular) and Fig. 3 (linear). Individual observations show only small variations from night to night, and thus combining the data from the separate nights, and averaging to the phase bins over orbital cycle is appropriate in order to increase the S/N ratio. Circular polarimetry (Fig. 2) shows both negative and positive polarization. Positive circular polarization is observed in the orbital phase interval $\Phi = 0.5{-}1.1$ in the B-band and between $\Phi = 0.3{-}1.1$ in the V-, R- and I-bands. The circular polarization reaches +7% near the phase $\Phi = 0.8$ in the B-band, +6% in the V- and I-bands, and +5% in the U- and R-bands. The negative circular polarization reaches -5% in the B-band ($\Phi = 0.3$), -4% in the I-band ($\Phi = 0.2$), -2% in the V- and (quite marginally) -1% in the R-band ($\Phi = 0.1$). In the U-band the negative circular polarization is almost negligible.

Figure 3 shows the phase binned linear polarization data, computed by vectorially averaging individual observations from the B-,V-, R-, and I-bands in order to increase the S/N ratio. U-band data is not combined with the data from the other wavelengths due to higher noise level in this band. The degree of the linear polarization is low: 3% at maximum and during most part of the orbital cycle polarization is less than 1%.

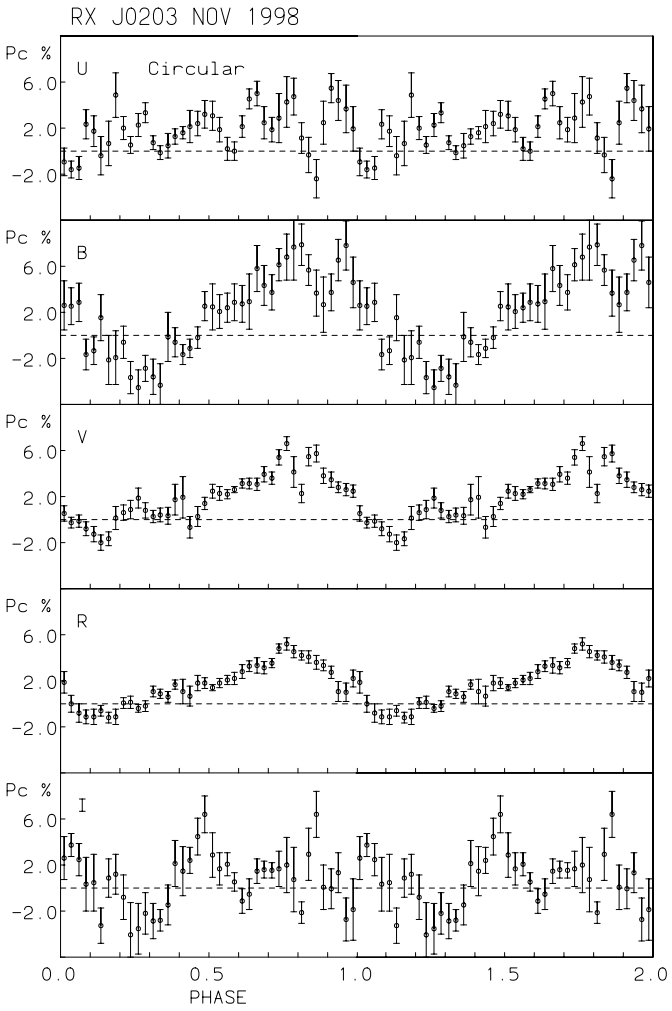

Fig. 2. Simultaneous circular polarization curves ($UBVRI$) of RX J0203.8+2959. Data obtained during 7 nights between 13/14 and 19/20 November 1998, has been averaged to 40 phase bins. Error bars correspond to the standard error of the mean ($\pm\sigma$).

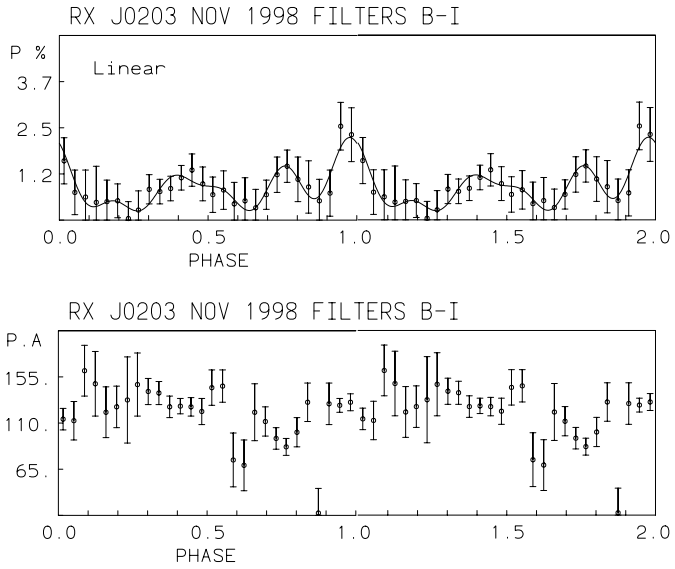

Fig. 3. Simultaneous linear polarization (top) and position angle (bottom) curves of RX J0203.8+2959 calculated by vectorially averaging the individual observations of B-, V-, R-, and I-bands. Data have been averaged to 28 phase bins. Error bars correspond to the standard error of the mean ($\pm\sigma$). The continous line is a Fourier fit with 5 harmonics of the orbital period.

The linear polarization shows pulses with defined position angle between the orbital phases $\Phi = 0.3-0.5$ and $\Phi = 0.95-1.05$. Both of these peaks coincide with the change of the sign in the circular polarization. A pulse-like feature is seen also near the phase $\Phi = 0.75$, but there are no zero crossings in the circular polarization near the same orbital phase. The linear polarization drops to low level at the phase $\Phi = 0.9$. A similar drop in polarization is also seen in the circular data in the U-, B-, and V-bands, almost near the same phase. This may be due to some unpolarized material (an accretion stream?) crossing our line of sight to the cyclotron emission area between orbital phases $\Phi = 0.90-0.95$. Earlier ROSAT X-ray observations by Schwarz et al. (1998) showed that during the short interval near photometric phase $\Phi = 0.9$ HRI-detectors had almost zero counts. Optical light curves (Fig. 1) do not reveal any drop in the flux level during the same orbital phase, however.

Comparing our polarization data to earlier ROSAT PSPC and HRI detectors data and HR1 hardness ratio, by Schwarz et al. (1998) (Fig. 16 in their paper; HR1 hardness ratio is defined as (H-S)/(H+S), where H and S are counts above and below 0.4 keV), it can be noticed that the soft X-ray component (HR1 ~ -0.8) is observed between the photometrical phases $\Phi = 0.0$ and $\Phi = 0.5$. The HR1 ratio changes rapidly after the phase $\Phi = 0.5$ from –0.8 to ∼0.0 and reaches at the phases $\Phi = 0.7-0.8$ its maximum, ∼0.5, at the same time when also the positive circular polarization has its maximum peak value. The soft X-ray component thus either disappears, or strongly reduces, when a linear pulse is seen and circular polarization changes its sign. After photometric phase $\Phi = 0.95$, HR1 hardnes ratio drops from hard to soft. This coincides with linear polarization pulse observed between the phases $\Phi = 0.95-1.05$, and may be connected to disappearing of the main emission region (positive pole). The two X-ray components, soft and hard, seen at different orbital phases, coinciding with a change from negative to positive circular polarization, suggest two pole accretion.

The wavelength dependences of the negative and the positive circular polarization are also slightly different. Furthermore, the positive circular polarization is observed when V-, R-, and I-bands have their maxima in brightness, whereas the negative circular polarization is seen during the phases ($\Phi = 0.1-0.4$) when the U- and B-light curves have their maxima. Also this favours a two accreting pole model.

3. The system geometry

The direction of the linearly polarized component of the cyclotron emission is perpendicular to the field. This information can be used for computing the inclination of the rotation axis with respect to our line of the sight in the dipole model approximation (Meggit & Wickramasinghe 1982; Liebert et al. 1982)

$$\cos\ i = \frac{\mathrm{d}\theta}{\mathrm{d}\phi}\ \sim\ \frac{\dot{\theta}P}{2\pi}. \qquad (2)$$

We have applied a standard least square fit method to calculate the rate of the change of the position angle $\dot{\theta}$ during two pulses, in order to estimate the orbital inclination i. Fits in the phase interval $\Phi = 0.30-0.48$ give inclination, when weighting according to inverse square of the standard error of each normal points, $i = 73^{\circ+13}_{-15}$. The broad pulse can be connected either with disappearance of the negative pole behind the limb of the white dwarf or appearance of the positive pole. This pulse may also has been affected by effects arising from possible overlap of the linear polarization from another accretion pole, which may also increase uncertainties in our inclination estimates.

During the other linear polarization pulse the least square fit (weighted according errors) to position angle data between orbital phases $\Phi = 0.91-1.05$ gives $i = 67^{\circ+21}_{-24}$. The observed variations in position angle are noisy, but not randomly scattered. They suggest (within given error estimates) high orbital inclination more probable solution than low inclination. Evidences of two accreting poles (see Sect. 2.2) also supports high inclination according Schwarz et al. (1998). Assuming orbital inclination $i \sim 70^{\circ}$, the lack of self-eclipses in the light curves would require a colatitude $\beta \leq 20^{\circ}$ for main accreting region. However, *if* there are more than one region accreting, the main accreting region may have self-eclipses if another emission region is seen during that time interval. By studying circular polarization curves (Fig. 2) it is obvious that possible self-eclipse of the main accretion region has quite short duration, because positive circular polarization is observed during most of the the orbital cycle.

By using formula given by Bailey & Axon (1981):

$$\cos\ 2\pi\phi_{\mathrm{o}} = \frac{1}{\tan\ i\ \tan\ \beta} \qquad (3)$$

where $2\phi_{\mathrm{o}}$ is the length of the phase interval where the sign of the circular polarization is reversed, and the active pole is far side of the white dwarf, we can estimate β. The circular polarization data (Fig. 2) show values of $\sim$0.4 (B-band) and $\sim$0.2 (V-, R, and I-bands) for $2\phi_{\mathrm{o}}$, which would then results values in the range from 50° to 24° for β, and correspondingly for negative pole values of β range from 155° to 130°.

4. Comparison with cyclotron model computations

We have reproduced the observed light curves and polarization variations by using the numerical modelling codes for cyclotron emission described in Piirola et al. (1987a,b, 1990, 1993). For the cyclotron fluxes and polarization dependence on the viewing angle α, the angle between the line of the sight and the magnetic field, we have used model grids given by Wickramasinghe & Meggit (1985) for constant high temperature $T_{\mathrm{shock}} = 10-40$ keV (originally in 10 degrees divisions) which we have further interpolated over whole range of viewing angle α for one degree divisions. These models predict the intensity of the cyclotron emission and linear and circular polarization from a point source for different viewing angles for each harmonics for a given optical depth parameter Λ and electron shock temperature T_{shock}.

The height of the emission region(s) is assumed to be very small compared to the radius of the white dwarf. The observations of ST LMi (Cropper 1986), BL Hyi (Piirola et al. 1987a), VV Pup (Piirola et al. 1990), for example, have shown that the height of the emitting regions, h, is very small in units of white dwarf radius, $h \leq 0.01\ R_{\mathrm{WD}}$. The orbital inclination is adopted to the value $i = 70^{\circ}$, which is near the estimates from the rate of change of the position angle during the two pulses (Sect. 3). The colatitudes and longitudes of the emission regions, extension of the emission regions in longitude and in colatitude are kept as free parameters.

The amount of polarization given by the constant temperature Wickramasinghe & Meggit (1985) models is often too high (see Cropper 1985; Piirola et al. 1987a,b, 1990). The inclusion of an unpolarized background emission is necessary in order to bring the polarization values into better agreement with the observations. We have adopted a colour dependence of the background comparable to relative flux ratios near $\Phi = 0.0$ in each band (lowest states during orbital cycle) to separate unpolarized background effects. Schwarz et al. (1998) found that the faint and the bright phase during the orbital cycle in RX J0203.8+2959 was dominated by blue continuum, where at least three separate components may contribute: optically thick cyclotron emission from accretion region, photospheric radiation of the white dwarf itself, and possible large fraction of reprocessed continuum radiation from the line emitting regions. Schwarz et al. (1998) also estimated that only 25% of total visual light observed during the high state originates from measured cyclotron flux. In our modelling the adopted background fluxes are in the B-, V-, and R-bands 3–4 times larger than the peak emission from pure cyclotron flux (depending on wavelength).

Calculations are made by dividing extended emission arcs into three separate strips, each consisting of 20 equidistant points along a line on the surface of the white dwarf, for which Stokes parameters Q, U, V and I are calculated independently, as an approximation for regions where volume elements do not obscure each other, and their contributions to total polarization and flux are summed together as a function of orbital phase. The geometric model which gives acceptable fits to our data for different temperatures T_{shock}, plasma parameter Λ values and for different harmonics numbers $\omega/\omega_{\mathrm{o}}$, by using value

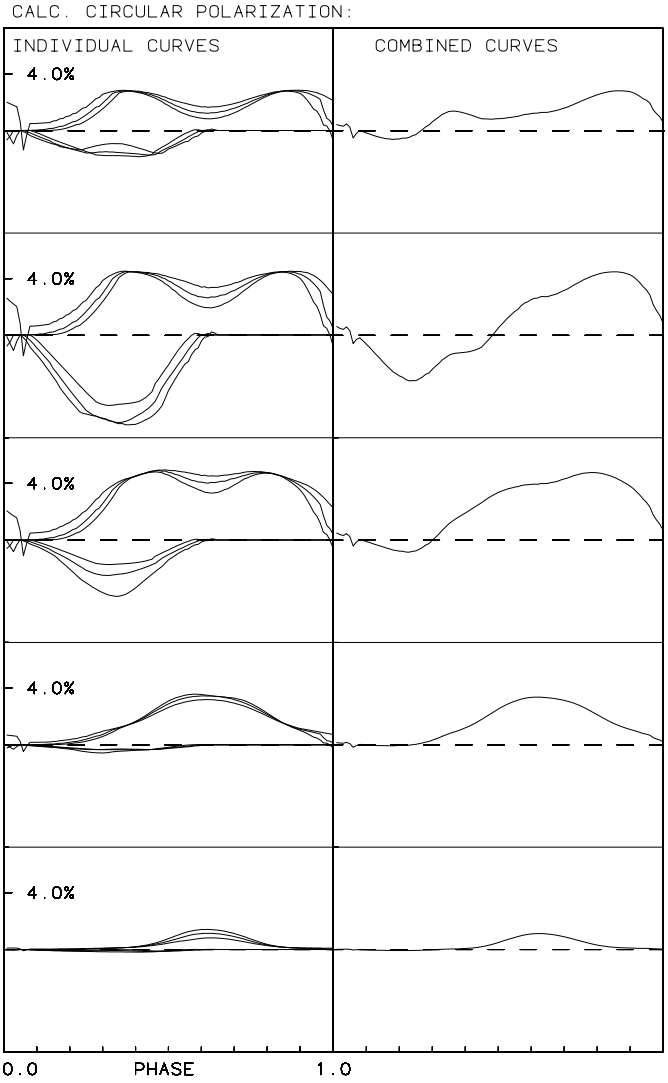

Fig. 4. Calculated circular polarization curves from orbital phase $\Phi = 0.0$ to $\Phi = 1.0$, by using parameters $i = 70°$, two extended emission regions between colatitudes $\beta = 20°-30°$ and $\beta = 120°-140°$, by 90° in longitude separated and both consisting of three strips, centered at colatitudes 20°, 30°, and 40° (positive region) and 120°, 130°, and 140° (negative region). Values $kT = 20\,\mathrm{keV}$, $\Lambda = 10^4$ and harmonic number ω/ω_c from 8 (top), 7, 6, 5 and 4 (bottom) are used for dominant positive circular polarization region. Correspondingly values for ω/ω_c from 7 (top), 6, 5, 4, and 3 (bottom), $kT = 10\,\mathrm{keV}$, $\Lambda = 10^5$ are applied for negative cirular polarization emission region. Left panel shows curves for individual emission strips and the right panel the combined polarization curves.

$i = 70°$ for orbital inclination, contains two extended emission regions, (separated 90° in longitude): positive (main) circular polarization region between colatitudes $\beta = 20°$ and 30° and the other region (negative polarization) between $\beta = 120°$ and 140°.

The general pattern of circular polarization variations over the orbital cycle (Fig. 2) is fairly well reproduced by the model, using cyclotron model parameters $kT_\mathrm{shock} =$ 20 keV, $\Lambda = 10^4$, and the harmonics 8, 7, 6, 5, and 4 in the $UBVRI$ bands, respectively (Fig. 4) for the main accretion region. These harmonics correspond to magnetic field of about 32–33 MG. The low S/N ratio in the U and I bands (Fig. 2) does not allow any detailed comparison of the phase dependent variations in U and I, but the amplitude level in these bands is roughly in accordance with the predictions from the model. The relative amount of negative circular polarization is largest in the blue, which points to the possibility of stronger magnetic field in the second, less active, pole. Our best fit, with $kT_\mathrm{shock} = 10$ keV and the harmonics (7), 6, 5, 4, and (3), in the $(U)BVR(I)$ bands, respectively for the negative circular polarization, corresponds to magnetic field of about 40–41 MG. These field estimates are in reasonable agreement with the value 38 ± 2 MG obtained by Schwarz et al. (1998). Tight constraints for the field strength can not be set based to our cyclotron model fittings, but varying a large range of harmonics with different temperatures and plasma parameters, we can say that harmonic numbers 3 or lower, are not able to predict well variations observed in the I-band, as well the harmonics clearly higher than 8 or 10, do not seem to give enough high polarization for B-band, setting the field range to be about 25–43 MG. Confirmed two-pole accretors, like VV Pup (Wickramasinghe et al. 1989), UZ For (Schwope et al. 1990), DP Leo (Cropper & Wickramasinghe 1993) and QS Tel (Schwope et al. 1995), have shown significantly different fields in two accreting regions. In some cases, nearly a factor of 2 difference has been observed between magnetic field strengths in different poles. The more strongly accreting pole has usually the weaker magnetic field.

The models predict brightness variations (Fig. 5) which are about three times smaller than observed and not that smooth. If we reduce the amount of unpolarized background, the relative flux variations increase, but then the polarization predicted by the model will be too high. The observed linear polarization pulses at phases 0.5 and 0.95 are well reproduced by the model (Fig. 6). The negative pole is near the limb at the phase 0.5. The minimum in the brightness near the phase $\Phi = 1.0$ is due to having both emission regions at self-eclipse by the white dwarf limb. The length of the extended accretion regions are not very strongly constrained. The fit to the observed smooth and asymmetric variations in circular polarization and flux, by using small and very short accretion regions is worse comparing to fitting by longitudinally extended emission regions. The short emission regions produce also a short-term, sharp linear pulse with too high peak value, whereas the longer emission regions give flatter and weaker linear polarization peaks (consistent with observations) when the angle between magnetic field and our line of the sight, α, is close $\sim$90°.

The best fit to observed data is achieved by assuming relatively long emission regions (tens of degrees in longitude). The length of the main emission region in our model shown in Figs. 4, 5, and 6 (60° in longitude) corresponds $\sim 1/3\,R_\mathrm{wd}$ in units of white dwarf radius. The asymmetry seen in our light (Fig. 1) and polarization curves (Fig. 2) of

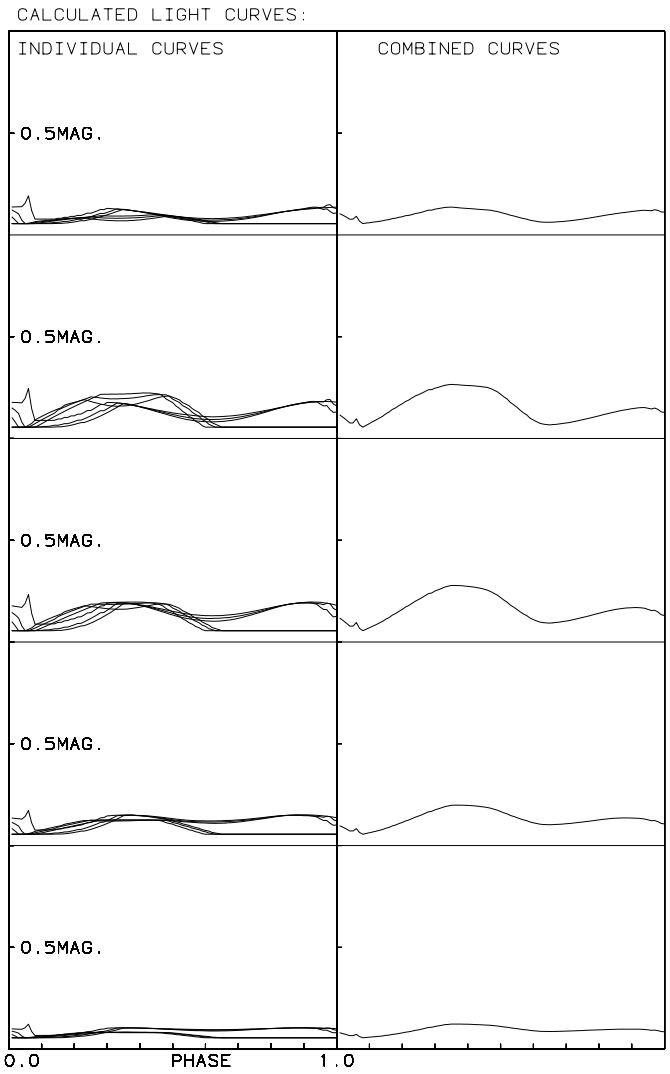

Fig. 5. By using the same parameters as in Fig. 4 (for circular polarization) the calculated light curves are presented.

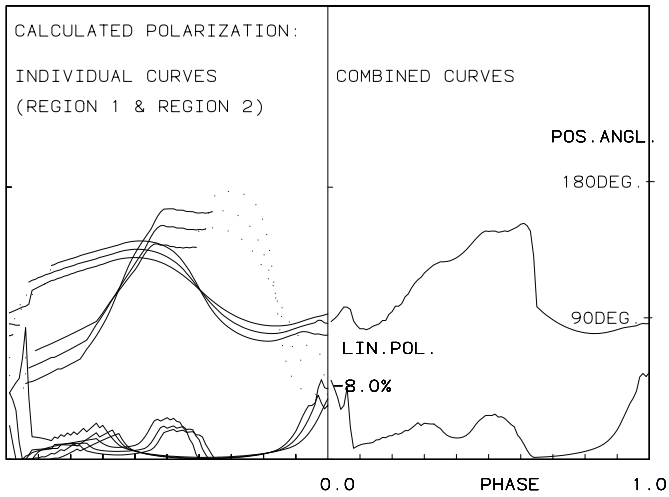

Fig. 6. Calculated linear polarization and position angle curves for harmonic number $\omega/\omega_c = 7$ for positive pole and harmonic $\omega/\omega_c = 6$ for negative pole. The other parameters are the same as for calculations in Figs. 4 and 5.

RX J0203.8+2959, suggests also that the cyclotron emission regions are longitudinally extended. This is in accordance with earlier modelling of cyclotron emission in AM Herculis stars. The assumption that the accretion takes place over a small spot near the magnetic pole in centered dipole field is showed to be too simplified. Longitudinally extended arc-shaped accretion region(s), slightly offset from the magnetic pole, have been proposed to explain the circular polarization curves in AM Herculis stars, see e.g.: Wickramashinge & Ferrario (1988), and Ferrario & Wickramasinghe (1990).

Observed polarization and brightness variations have been succesfully modelled by using extended emission regions, for example, in ST LMi (Ferrario et al. 1989; Ferrario et al. 1993; Cropper & Horne 1994), DP Leo (Schmidt 1988; Cropper & Wickramasinghe 1993); V347 Pav (Bailey et al. 1995; Ramsay et al. 1996; Potter et al. 2000). The extension of emission regions have been estimated to be, for example: $0.25\,R_{\rm wd}$ (Wickramasinghe 1988), $0.3\,R_{\rm wd}$ (UZ For in high state, Schwope et al. 1990), $0.5\,R_{\rm wd}$ (DP Leo, Schmidt 1988) or extended from 15° to ∼100° in longitude (V834 Cen, Cropper 1989; ST LMi, Cropper & Horne 1994; VV Pup, Piirola et al. 1990; DP Leo, Cropper & Wickramasinghe 1993; EV UMa, Hakala et al. 1994). Recent X-ray observations have also shown that hard X-ray emission regions in systems BL Hyi (Wolff et al. 1999) and V2301 Oph (Steinman-Cameron et al. 1999) have extension of 45°–50° in longitude.

Although that our model is able to produce the observed variations in polarization acceptable well (Figs. 4, 5, and 6), we can not assert that our solution is unique. The model fits are depending on several parameters, such as orbital inclination, (data favours high inclination, see Sect. 2.2) and choice of the correct electron shock temperature $T_{\rm shock}$ and plasma parameter Λ (values $kT = 20$ keV are adopted from Schwarz et al. 1998 fits to ROSAT-data).

5. Conclusions

We have observed RX J0203.8+2959 and collected a large amount of circular and linear polarimetric and photometric data covering well the orbital phase. A rise of positive circular polarization is observed near the same orbital phases as the change in X-ray spectrum HR1 hardness ratio in 1994 during ROSAT observations. Negative circular polarization is observed at the same orbital phase when the soft X-ray component is seen (Schwarz et al. 1998). Linear polarization show pulses at the orbital phases when the sign of the circular polarization is reversed. Two pulses coincide with the change in the X-ray spectrum. Observed polarization variations favour a two-pole accretion instead of one accreting pole model. The position angle variations suggest relatively high values for the inclination angle of the white dwarf spin axis, $i \sim 70°(\pm 20°)$.

Acknowledgements. This work was supported by the Finnish Academy of Sciences and Letters (Academia Scientiarum

Fennica). We thank the referee for profound comments, which have improved our manuscript. We thank also Dr. C. Flynn for a reading of the manuscript.

References

Bailey, J., & Axon, D. J. 1981, MNRAS, 194, 187
Bailey, J., Ferrario, L., Wickramasinghe, D. T., Buckley, D. A. H., & Hough, J. 1995, MNRAS, 272, 579
Beuermann, K., & Thomas, H. C. 1993, Adv. Space Res., 13, 115
Cropper, M. S. 1985, MNRAS, 212, 709
Cropper, M. S. 1986, MNRAS, 222, 853
Cropper, M. 1989, MNRAS, 236, 935
Cropper, M. S., & Wickramasinghe, D. T. 1993, MNRAS, 260, 696
Cropper, M., & Horne, K. 1994, MNRAS, 267, 481
Ferrario, L., Wickramasinghe, D. T., & Tuohy, I. R. 1989, ApJ, 341, 327
Ferrario, L., & Wickramasinghe, D. T. 1990, ApJ, 357, 582
Ferrario, L., Bailey, J., & Wickramasinghe, D. T. 1993, MNRAS, 262, 285
Hakala, P. J., Piirola, V., Vilhu, O., Osborne, J. P., & Hannikainen, D. C. 1994, MNRAS, 271, L41
Liebert, J., Stockmann, H. S., Williams, R. E., et al. 1982, ApJ, 256, 594
Meggit, S. M. A., & Wickramasinghe, D. T. 1982, MNRAS, 198, 71
Piirola, V. 1973, A&A, 27, 383
Piirola, V. 1988, in Polarized Radiation of Circumstellar Origin, ed. G. V. Coyne, A. M. Magalhaes, & A. F. J. Moffat (Vatican City: Vatican Press), 735
Piirola, V., Reiz, A., & Coyne, G. V. 1987a, A&A, 185, 189
Piirola, V., Reiz, A., & Coyne, G. V. 1987b, A&A, 186, 120
Piirola, V., Reiz, A., & Coyne, G. V. 1990, A&A, 235, 245
Piirola, V, Hakala, P., & Coyne, C. V. 1993, ApJ, 410, L107
Potter, S., Cropper, M., & Hakala, P. J. 2000, MNRAS, 315, 423
Ramsay, G., Cropper, M., Wu, K., & Potter, S. 1996, MNRAS, 282, 726
Schmidt, G. D. 1988, in Polarized Radiation of Circumstellar Origin, ed. G. V. Coyne, A. M. Magalhaes, & A. F. J. Moffat (Vatican City: Vatican Press), 85
Schwarz, R., Schwope, A. D., Beuermann, K., et al. 1998, A&A, 338, 465
Schwope, A. D., Beuermann, K., & Thomas, H. C. 1990, A&A, 230, 120
Schwope, A. D., Thomas, H. C., Beuermann, K., et al. 1995, A&A, 293, 764
Steinman-Cameron, T. Y., & Imamura, J. N. 1999, ApJ, 515, 404
Wickramashinge, D. T., & Meggit, S. M. A. 1985, MNRAS, 214, 605
Wickramasinghe, D. T. 1988, in Polarized Radiation of Circumstellar Origin, ed. G. V. Coyne, A. M. Magalhaes, & A. F. J. Moffat (Vatican City: Vatican Press), 3
Wickramasinghe, D. T., & Ferrario, L. 1988, ApJ, 334, 412
Wickramasinghe, D. T., Ferrario, L., & Bailey, J. 1989, ApJ, 342, L35
Wolff, M. T., Wood, K. S., Imamura, J. N., Middleditch, J., & Steinman-Cameron, T. Y. 1999, ApJ, 526, 435